

Effects of Carrier Confinement and Intervalley Scattering on Photoexcited Electron Plasma in Silicon

A. Sieradzki · Z. T. Kuznicki

Received: 21 February 2013 / Accepted: 22 May 2013 / Published online: 4 June 2013
© The Author(s) 2013. This article is published with open access at Springerlink.com

Abstract The ultrafast reflectivity of silicon, excited and probed with femtosecond laser pulses, is studied for different wavelengths and energy densities. The confinement of carriers in a thin surface layer delimited by a nanoscale Si-layered system buried in a Si heavily-doped wafer reduces the critical density of carriers necessary to create the electron plasma by a factor of ten. We performed two types of reflectivity measurements, using either a single beam or two beams. The plasma strongly depends on the photon energy density because of the intervalley scattering of the electrons revealed by two different mechanisms assisted by the electron–phonon interaction. One mechanism leads to a negative differential reflectivity that can be attributed to an induced absorption in X valleys. The other mechanism occurs, when the carrier population is thermalizing and gives rise to a positive differential reflectivity corresponding to Pauli-blocked intervalley gamma to X scattering. These results are important for improving the efficiency of Si light-to-electricity converters, in which there is a possibility of multiplying carriers by nanostructurization of Si.

Keywords Ultrafast processes · Electron–hole plasma · Nanostructured silicon

A. Sieradzki
Institute of Physics, Wrocław University of Technology, Wybrzeże
Wyspiańskiego 27,
50-370 Wrocław, Poland

A. Sieradzki (✉)
Institut de Physique et Chimie des Matériaux de Strasbourg, UMR
7504, CNRS, Université de Strasbourg, BP 43, 23 rue du Loess,
67034 Strasbourg, France
e-mail: adam.sieradzki@pwr.wroc.pl

Z. T. Kuznicki
Photonic Systems Laboratory, Pôle API Parc d’Innovation,
Boulevard Sébastien Brant, BP 10413,
67400 Illkirch, France

Generating an electron plasma in heavily-doped or photoexcited silicon is important for optoelectronic and photonic devices [1]. For example, creating plasma with light in the visible range would increase the light-to-electricity conversion efficiency. It is therefore useful to know the factors that enhance or hinder high carrier density generation [2, 3]. In semiconductors and metals, the dielectric response function in the optical range is described mainly by intraband and interband transitions. Understanding the dynamics of the two transitions is important because they determine the fundamental optoelectronic properties of semiconductor devices depending on the generation, injection, and transport of conduction electrons [4]. Free-carrier scattering by surface plasmons in metal or metal-like nanostructures control dynamics of light emitting devices and, in general, light–matter interactions with lattice and free-carrier contributions. In the case of Si, a quasimetallic state can be produced at large densities of excited carriers [5]. This state is due to the creation of plasma with carrier density up to 10^{22} cm^{-3} , which has characteristics of a Drude-like electron gas [6].

Previous ultrafast experiments performed on the dense-free carrier gas in Si have shown that the critical carrier density N_c depends on pulse duration and laser fluence [7]. On the nanosecond [8–11] and picosecond [12–16] time scales, a solid to liquid phase transition has been reported and explained in terms of thermal processes. However, studies with femtosecond laser pulses have shown an ultrafast phase transition from the solid to a metallic liquid phase that is too fast to be explained by thermal processes [17–19]. Several attempts have been made to explain this ultrafast plasma generation in terms of lattice instability induced by excess carriers [20–22]. Other explanations have been based on the dependence of plasma parameters on excitation intensity [23, 24]. A detailed analysis of the time-resolved reflectivity in Si has shown that an extremely dense electron plasma can be generated by two-photon absorption [25]. In the present work, using ultrafast laser

spectroscopy, we look at two aspects of carrier dynamics in Si: spatial confinement and intervalley scattering processes.

We show that N_c , for which the electron plasma is formed, is reduced by a factor of ten, if the electrons are confined above a buried amorphous Si layer made by ion implantation [26]. We also show that, depending on the exciting wavelength, $\Gamma \rightarrow X$ intervalley electron scattering leads to a complex carrier dynamics that can disadvantage the creation of the electron plasma.

Two Si samples have been studied. The first one (S_A) is undoped (technically intrinsic) with a residual impurity concentration less than 10^{15} cm^{-3} . The second one (S_B) has an amorphous layer buried by implantation and n-doping of 10^{20} cm^{-3} . The $2 \times 2 \text{ cm}^2$ sample was cut from a 4-in diameter p-type (boron, $5 \cdot 10^{15} \text{ cm}^{-3}$), (001) oriented FZ Si wafer 450 μm thick. Heavy n-type doping (phosphorous) was done by diffusion from a planar surface source at 850 $^\circ\text{C}$. The sacrificial SiO_2 electronic passivation controlled the surface recombination rate [27]. Figure 1 shows an electron microscopic image of the S_B sample. It was designed to induce a high carrier density near the surface of the silicon wafer by preventing in-depth carrier diffusion.

Photogenerated free-carriers are confined above the buried nanoscale Si-layered system. The layered design of the cell was chosen for two reasons: first, to confine a large electron population and next to well define and precisely localize the potential barriers of the nanoscale separation that determine the electronic and optical behaviors of the device. The resulting density of the electron gas can exceed 10^{22} cm^{-3} [28].

In the experiments, we have used an amplified laser system from Spectra physics (Tsunami and Spitfire). The oscillator (Tsunami) delivers pulses at 800 nm with 80 fs duration, a rate of 82 MHz, and an average output power of 600 mW. A continuous laser (Millenia) is used to pump the Tsunami cavity, and another pulsed laser (Evolution X) is used to pump the regenerative amplifier cavity (Spitfire). The pulses are amplified using a regenerative amplifier with a Ti:sapphire slab as a gain medium. The output of the amplifier delivers an average power of $\sim 650 \mu\text{W}$, which corresponds to an energy of 200 $\mu\text{J/pulse}$, which have a pulse duration of 150 fs at 5 kHz.

We performed two types of reflectivity measurements, using either a single-beam or two-beams. In the single-beam experiment, the reflectivity $R(\lambda, E_{\text{abs}})$ of p-polarized femtosecond pulses was measured as a function of wavelength λ and absorbed energy E_{abs} . The laser beam was directed onto the sample at an angle of incidence on the sample of 15° to the vertical and was focused to an almost circular spot of 40 μm diameter by an achromatic lens with a focal length of 75 mm; the spot size was determined with a microscope reticule.

The quantity of interest is the static differential reflectivity $(\Delta R/R)_{\text{stat}} = [R(\lambda, E_{\text{abs}}) - R(\lambda, E_{\text{abs}} \approx 0)] / R(\lambda, E_{\text{abs}} \approx 0)$. The

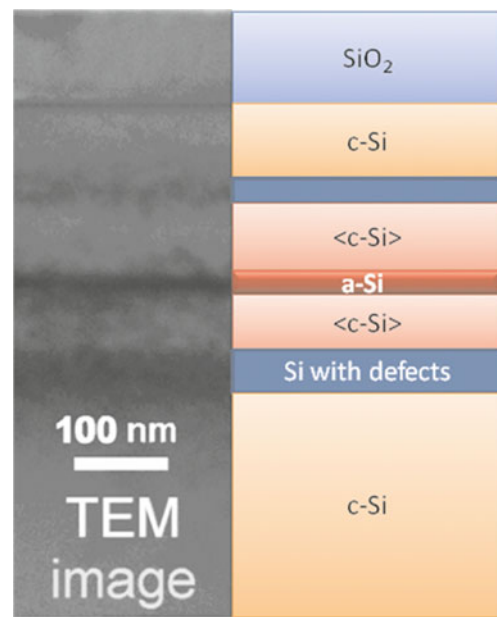


Fig. 1 Cross section of the investigated silicon structures (*left*), electron microscope image of the nanoscale Si-layered system (sample S_B), and (*right*) a labeled schematic of the system shown in the TEM, where a-Si: amorphous Si, c-Si: relaxed crystalline Si, <c-Si>: strained crystalline Si

measurements were performed at the fundamental wavelength $\lambda = 794 \text{ nm}$ and at the half wavelength $\lambda = 397 \text{ nm}$, obtained by second harmonic generation in a 5 mm thick beta barium borate crystal. The static reflectivity was measured with calibrated photodiodes by recording its average value from 100 laser shots. In this static experiment, the absorbed pump energy E_{abs} was varied with a half-wave plate coupled with an optical polarizer and was measured by a wattmeter placed just before the sample surface. The laser pulse energy used in this experiment was set below the ablation threshold value. In the two-beam (pump-probe) experiment, we measured the normalized differential reflectivity: $\Delta R(\lambda, \tau, E_{\text{abs}}) / R_0(\lambda, E_{\text{abs}})$ as a function of pump-probe delay τ . The probe is a supercontinuum generated in a sapphire crystal, providing a dispersion-compensated spectrum in the 490–650 nm range.

Figure 2 shows the reflectivity of the laser beam as a function of E_{abs} for several situations. Figure 2a shows $(\Delta R/R)_{\text{stat}}$ for sample S_A at $\lambda = 397$ and $\lambda = 794 \text{ nm}$. Figure 2b shows the same quantity for sample S_B at $\lambda = 397 \text{ nm}$. The behavior of these curves is similar; first, they decrease as absorbed energy increases to a broad minimum, that is next followed by an increase of $(\Delta R/R)_{\text{stat}}$ to positive values. This nonmonotonic variation is related to the creation of dense electron plasma.

Experimentally, the large increase of R demonstrates that free-carriers dominate the optical response due to a transformation from the semiconducting solid phase to a metallic liquid one. The $N_c(\lambda)$, corresponding to the onset of the

plasma, is related to the absorbed energy, for which the observed differential reflectivity $(\Delta R/R)_{\text{stat}}$ equals zero. In Fig. 2a, the value N_c is indicated for both wavelengths used. As seen in Fig. 2b, N_c is reduced by a factor of 10 at $\lambda=397$ nm for the nanostructured sample. This behavior is well-described by a Drude-like plasma, with a complex dielectric function $\epsilon_{\text{intra}}(\omega, N_c)$:

$$\epsilon_{\text{intra}} = \epsilon_B - \frac{\omega_p^2}{\omega(\omega + i\gamma)} \tag{1}$$

where, ω and $\omega_p = \sqrt{N} e^2/\epsilon_0 m_e^*$ are the incident and plasma frequencies, N the density of carriers, m_e^* the effective electron mass, ϵ_B the background dielectric function, and γ the plasma damping, which corresponds to the inverse Drude damping time τ_D . For a strongly damped plasma ($\omega\tau_D \ll 1$), the reflectivity minimum tends to the value of the unperturbed solid, which corresponds to $(\Delta R/R)_{\text{stat}}=0$. For a weakly damped plasma ($\omega\tau_D \gg 1$), the reflectivity approaches zero, and $(\Delta R/R)_{\text{stat}}$ decreases significantly. It is well-known that for intense excitation, the bandgap renormalization also starts to play an important role. Often, this process is treated as a rigid shift of the band structure resulting in a narrowing of the energy gap proportional to the cube root of the density. However in our case, this effect is too weak to cause a direct band gap transition.

Figure 2c shows the calculated reflectivity as a function of N_c for two different damping rates γ . In Eq. (1), the reflectivity at the minimum and the slope of the rising curve are determined by the magnitude of the imaginary part of

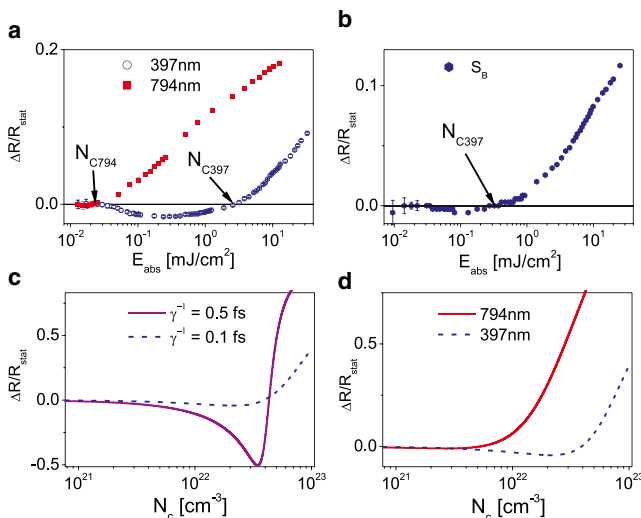


Fig. 2 Creation of electron plasma in intrinsic, doped, and nanostructured Si. **a** Reflectivity change of pure/intrinsic Si (sample S_A) as a function of absorbed energy for wavelengths 397 and 794 nm. **b** Reflectivity of nanostructured Si (S_B) as a function of absorbed energy for $\lambda=397$ nm. Modeling of the reflectivity of pure Si as a function of the electron plasma density is shown in **c** for different damping constants ($\gamma=10^{16}$; 2×10^{15}) and in **d** for different wavelengths

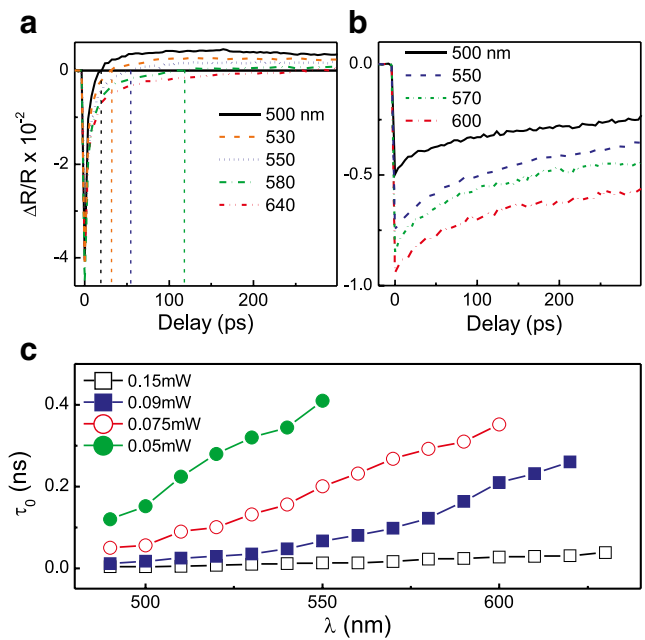


Fig. 3 Time-resolved reflectivity of Si in the visible spectrum. The pump wavelength and energy density are set at: **a** $\lambda_{\text{pump}}=397$ nm; $E_{\text{abs}}=2.3$ mJ/cm² and **b** $\lambda_{\text{pump}}=794$ nm; $E_{\text{abs}}=2.2$ mJ/cm². **c** Variation of the time τ_0 at which the reflectivity changes sign $\Delta R(\lambda, \tau_0, E_{\text{abs}})/R_0=0$ (dashed lines in 3a) versus probe wavelengths for different pump intensities

ϵ_{intra} , which depends on the damping constant. For greater damping, the minimum of $(\Delta R/R)_{\text{stat}}$ is less contrasted. For low carrier densities, the main source of scattering comes from carrier-impurity scattering. In the plasma regime, carrier-carrier collisions dominate [29, 30]. Figure 2d shows the reflectivity calculated as a function of N for the two wavelengths (397 and 794 nm). The onset of the plasma clearly shifts to lower carrier densities at longer wavelength excitation as is observed in Fig. 2a. This is due to the fact that for a shorter pumping wavelength, there is an additional channel for carrier relaxation that inhibits formation of the

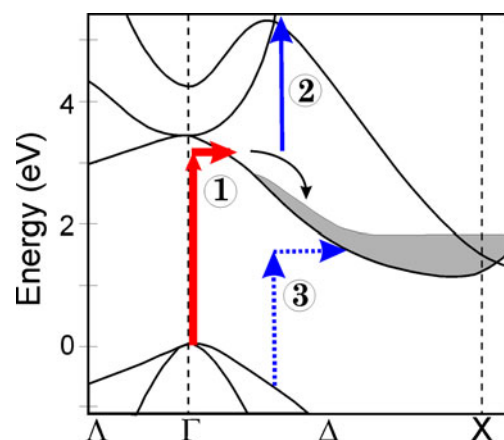


Fig. 4 Carrier dynamics of in Si excited with photons at $\lambda_{\text{pump}}=397$ nm. Intervalley scattering (I), induced absorption (2), and thermalization (3) of carriers

plasma. This channel is the intervalley scattering process discussed in the following.

Figure 3 shows the differential reflectivity of sample S_A (pure Si) for a pump wavelength $\lambda_{\text{pump}}=397$ nm (Fig. 3a), with an excitation density $E_{\text{abs}}=2.3$ mJ/cm² and $\lambda_{\text{pump}}=794$ nm (Fig. 3b) with $E_{\text{abs}}=2.2$ mJ/cm². For $\lambda_{\text{pump}}=397$ nm, $\Delta R(\lambda, \tau, E_{\text{abs}})/R_0(\lambda)$ is first negative than increases with a crossing point ($\Delta R/R_0=0$), which shifts to longer time delays, when the wavelength increases. For $\lambda_{\text{pump}}=794$ nm, all curves remain negative during the same time intervals.

We attribute the dynamics observed for $\lambda_{\text{pump}}=397$ nm to two different mechanisms shown in Fig. 4. They both result from the excitation of a nonthermal carrier population in the X valley via a $\Gamma \rightarrow X$ intervalley process (process 1 in Fig. 4), similar to the mechanism occurring in GaAs [31]. These intervalley transitions are assisted by the scattering of longitudinal optical phonons with energies $E_{\text{LO}}=63$ meV, immediately after pump excitation. The carrier population is transferred to the X valley, where it thermalizes, but the plasma can first be excited to higher energy states (process 2 in Fig. 4). The corresponding probe reflectivity therefore decreases. At later times, the carriers thermalizing in the X valley can also be observed from the Γ valley via a Pauli-blocking of the intervalley scattering (process 3 in Fig. 4), resulting in increased reflectivity. This process, which takes place at later times, occurs for lower photon energies because of the dispersion of the top valence band and the Γ and X conduction band points. Carrier thermalization in the X valley can therefore be “visualized” by considering the time τ_0 , for which the reflectivity at each wavelength changes sign, i.e., for which $\Delta R(\lambda, \tau_0, E_{\text{abs}})/R_0=0$. In Fig. 3c, the variation of τ_0 is plotted in the spectral range 490–630 nm for four absorbed energy densities. For a given wavelength, τ_0 decreases when the density of pump energy increases. This is due to the fact that carrier thermalization is density-dependent because their scattering cross section increases with electron temperature (as the square of the temperature in the case of a Fermi liquid).

In conclusion, we find that by combining dense electron gas effects with geometrical confinement, it is possible to obtain an additional parameter for manipulating electron energy levels in semiconductors with an indirect bandgap. It is shown that the critical energy density necessary to photoinduce a free-carrier plasma in Si is reduced in a nanoscale Si-layered system. $\Gamma \rightarrow X$ intervalley scattering dominates reflectivity in the visible. This mechanism is associated either with induced absorption (decreased reflectivity) or a Pauli-blocking process (increased reflectivity), depending on the photon energy. This new insight into an extremely dense electron gas in silicon should lead to additional applications of silicon in optoelectronics

and photonics in general and to the light-to-electricity conversion in particular.

Acknowledgments The authors thank the Region of Alsace, France for its financial support under project no. 07/928/065. We are grateful to J.-Y. Bigot and M. Albrecht of the IPCMS in Strasbourg for helping with experiments and useful discussions.

Open Access This article is distributed under the terms of the Creative Commons Attribution License which permits any use, distribution, and reproduction in any medium, provided the original author(s) and the source are credited.

References

- (2010) Nature Photonics 4, 491
- Huber R, Tausser F, Brodschelm A, Bichler M, Abstreiter G, Leitenstorfer A (2001) Nature 414:286
- Chemla DS, Shah J (2001) Nature 411:549
- Sundaram SK, Mazur E (2002) Nat Mater 1:217
- Goldman JR, Prybyla JA (1994) Phys Rev Lett 72:1364
- Sokolowski-Tinten K, Bialkowski J, Cavalleri A, von der Linde D, Oparin A, Meyer-ter-Vehn J, Anisimov SI (1998) Phys Rev Lett 81:224
- Dachraoui H, Husinsky W (2006) Phys Rev Lett 97:107601–1
- Yoffa EJ (1980) Phys Rev B 21:2415
- Preston JS, van Driel HM (1984) Phys Rev B 30:1950
- Hoai TX, Duong PH, Thanh DX, Nhung TH, Phan HK (1990) Phys Rev B 41:3638
- Lowndes DH, Jellison GE, Wood RF (1982) Phys Rev B 26:6747
- Liu JM, Kurz H, Bloembergen N (1982) Appl Phys Lett 41:643
- von der Linde D, Fabricius N (1982) Appl Phys Lett 41:991
- Lompré L-A, Liu J-M, Kurz H, Bloembergen N (1984) App Phys Lett 44:3
- van Driel HM (1987) Phys Rev B 35:8166
- Rasolt M, Kurz H (1985) Phys Rev Lett 54:722
- Shank CV, Yen R, Hirlimann C (1983) Phys Rev Lett 50:454
- Sjodin T, Petek H, Dai H-L (1998) Phys Rev Lett 81(5664)
- Ashitkov SI, Ovchinnikov AV, Agranat MB (2004) JETP Lett 79:529
- Combescot M, Bok J (1982) Phys Rev Lett 48:1413
- Stampfli P, Bennemann KH (1990) Phys Rev B 42:7163
- Silvestrelli PL, Alavi A, Parrinello M, Frenkel D (1996) Phys Rev Lett 77:3149
- Hulin D, Combescot M, Bok J, Migus A, Vinet JY, Antonetti A (1984) Phys Rev Lett 51:1998
- Murnane MM, Kapteyn HC, Falcone RW (1989) Phys Rev Lett 62:155
- Sokolowski-Tinten K, von der Linde D (2000) Phys Rev B 61:2643
- Kuznicki ZT (2003) Generation Photovoltaics for High Efficiency Through Full Spectrum Utilization. Ch. 8. In Luque A, Marti A (ed) 3rd. Institute of Physics Publishing, Bristol, UK
- Kuznicki ZT, Ley M (2003) Appl Phys Lett 82:4241
- Jellison GE, Withrow SP, McCamy JW, Budai JD, Lubben D, Godbole MJ (1995) Phys Rev B 52:14607
- Combescot M, Combescot R (1987) Phys Rev B 35:7986
- Sernelius BE (1991) Phys Rev B 43:7136
- Bigot J-Y, Portella MT, Schoenlein RW, Cunningham JE, Shank CV (1990) Phys Rev Lett 65:3429